Journal of Molecular Graphics and Modelling 44 (2013) 70–80

Contents lists available at ScienceDirect

Journal of Molecular Graphics and Modelling

journal homepage: www.elsevier.com/locate/JMGM

Conserved water mediated H-bonding dynamics of Ser117 and Thr119 residues in human transthyretin–thyroxin complexation: Inhibitor modeling study through docking and molecular dynamics simulation

Avik Banerjee, Hridoy R. Bairagya, Bishnu P. Mukhopadhyay*, Tapas K. Nandi, Deepak K. Mishra

Department of Chemistry, National Institute of Technology-Durgapur, Durgapur, West Bengal 713209, India

ARTICLE INFO

Article history:
Accepted 29 April 2013
Available online 14 May 2013

Keywords:
Human transthyretin
Amyloid
Molecular dynamics simulation
Ligand modeling
Docking

ABSTRACT

Transthyretin (TTR) is a protein whose aggregation and deposition causes amyloid diseases in human beings. Amyloid fibril formation is prevented by binding of thyroxin (T4) or its analogs to TTR. The MD simulation study of several solvated X-ray structures of apo and holo TTR has indicated the role of a conserved water molecule and its interaction with T4 binding residues Ser117 and Thr119. Geometrical and electronic consequences of those interactions have been exploited to design a series of thyroxin analogs (Mod1–4) by modifying 5′ or 3′ or both the iodine atoms of thyroxin. Binding energy of the designed ligands has been calculated by docking the molecules in tetrameric structure of the protein. Theoretically investigated pharmacological parameters along with the binding energy data indicate the potentiality of 3′,5′-diacetyl-3,5-dichloro-L-thyronine (Mod4) to act as a better inhibitor for TTR-related amyloid diseases.

1. Introduction

Human transthyretin (hTTR) acts as a primary transporter of thyroxin (T4) hormone in cerebrospinal fluid (CSF). Under physiological condition 10–25% T4 binds to TTR in blood plasma [1]. It also plays an important role in retinol (vitamin A) transportation on binding with retinol-binding protein (RBP) [2–5]. Several types of small molecules like natural products (e.g., resveratrol), drugs (e.g., diflunisal, flufenamic acid) and toxins bind to TTR [3,6]. The protein may play some role in sweeping up the toxic and foreign compounds from bloodstream [7] and in the pathogenesis of Alzheimer's disease by scavenging A-β peptide [8].

Normally, hTTR circulates in blood as a soluble homotetramer (55 kDa), but in some cases it polymerizes to form insoluble toxic amyloid fibrils and deposit in the extracellular spaces causing several diseases like familial amyloid cardiomyopathy (FAC), senile systemic amyloidosis (SSA), and familial amyloid polyneuropathy (FAP) [9]. In SSA and FAC, wild type TTR amyloids deposit on the cardiac and other tissues [10–12], whereas the mutant TTRs are involved in FAP and affect the nervous system, heart and choroid plexus [13–15]. Amyloid fibril aggregation causes cardio-myopathies, systemic and central neuropathies, etc. [16,17].

Till now no effective therapy is available for TTR related amyloidoses. The existing treatment is only the liver transplantation. However, recently some drugs, e.g., diflunisal, diclofenac and tafamidis [18,19] are used for TTR related amyloid diseases. Several biochemical evidences reveal that the amyloid fibril formation is prevented by binding of TTR with T4 [20]. But excess use of T4 can cause hyperthyroidism and enhance both osteoblastic and osteoclastic activities in cortical and trabecular bone [21]. Further, the detail interaction of T4 with TTR has also been illustrated in the different crystallographic structures of their complexes (PDB code: 2ROX, etc.). So the associative mode of interaction in the complexing mechanism may be used as a strategy for inhibitor design. In the tetrameric structure of TTR, the central channel has two funnel shaped binding sites for the natural ligands (Fig. 1A) and other small molecules [2,3,6,7]. Each binding site consists of three small depressions, which are termed as halogen binding pockets (HBPs). The outermost pocket (HBP-1) is surrounded by the side chains of Met13, Lys15, Thr106 and Ala108 [22]. Central pocket (HBP-2) is formed by Lys15, Leu17, Ala108, Ala109 and Leu110. The hydroxyl groups of Ser117, Thr119, carbonyl groups of Ser117,

Abbreviations: hTTR, human transthyretin; T4, thyroxin; CSF, cerebrospinal fluid; RBP, retinol-binding protein; FAC, familial amyloid cardiomyopathy; SSA, senile systemic amyloidosis; FAP, familial amyloidotic polyneuropathy; HBP, halogen binding pocket; Mod, modified; MD, molecular dynamics; ns, nano-second; ps, pico-second; fs, femto-second; K, Kelvin; TPSA, total polar surface area.

* Corresponding author. Tel.: +91 0343 2547074; fax: +91 0343 2547375/2546753.
E-mail address: bpmk2@yahoo.com (B.P. Mukhopadhyay).

1093-3263/$ – see front matter © 2013 Elsevier Inc. All rights reserved.
http://dx.doi.org/10.1016/j.jmgm.2013.04.010

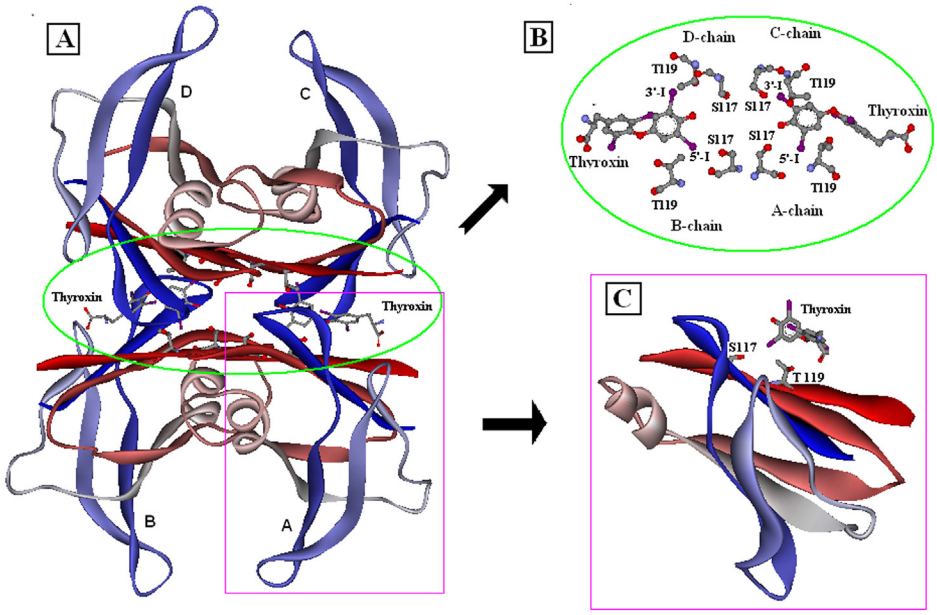

Fig. 1A. Three-dimensional structure of thyroxin bound human tarnsthyretin (tetramer) (PDB code: 1ICT) is shown in (A). Thyroxin bound monomeric transthyretin is shown in (B). Closer look at the inner core of the thyroxin binding cavity is shown in (C).

Thr118, Ala108 and main chain NH groups of Thr119, Ala109 and Leu110 residues form HBP-3 pocket (Fig. 1B). Thyroxin seems to interact with Glu54 [22]. In the X-ray structures, presence of one conserved water molecule at the ligand binding site near Ser117 and Thr119 residues seem to be interesting [23].

So, the presence of water molecules and their interaction at thyroxin binding sites of the unliganded simulated TTR structures may put forward some rational clues on the structural topology of thyroxin (T4) like inhibitors. The hydration susceptibility of T4 binding residues (Ser117 and Thr119) and their dynamics have encouraged us to design some thyroxin analogs. Drug-likeness of those molecules (T4-analogs) can also be judged by computing their molecular properties.

2. Materials and methods

The X-ray crystal structures of human transthyretin [3,23–27] were taken from RCSB Protein Data Bank [28]. The crystallographic and structural information (resolution, *R*-value, number of protein and water molecules in the asymmetric unit, ligands, etc.) of TTR have been included in Table 1. All these structures were found to crystallize as dimer (A and B molecule in the asymmetric unit) and the average temperature factor of B-molecule seem to be higher (~2–7 Å^2) than A-molecule. Swiss PDB Viewer Program [29] was used to separate the A-molecule and construct different structural models for solvation, energy minimization and MD simulation studies.

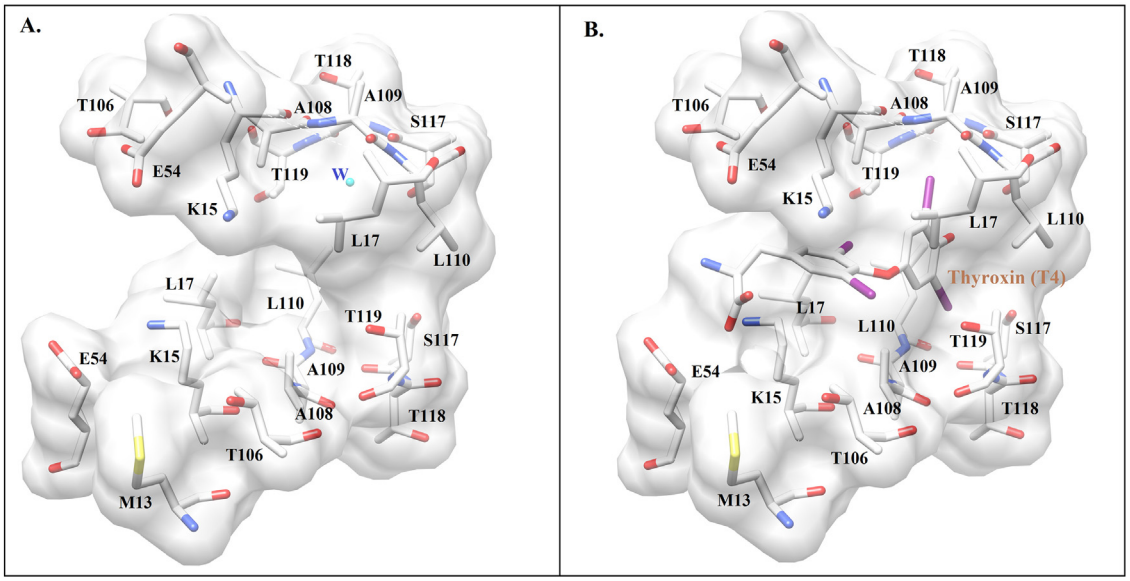

Fig. 1B. The thyroxin (T4) binding pocket of human tarnsthyretin: (A) The occupation of water molecule (W) in the T4 binding pocket (B) occupation of thyroxin in its pocket.

Table 1
Surveyed crystal structures of human-transthyretin protein.

PDB IDs (year)	Resolution (Å)	*R*-value (obs)	Molecules in the assym. unit	No of water molecules	Ligand	Reference
1F41 [a] (2000)	1.30	0.188	2	186	–	[23]
2QGB (2007)	1.40	0.167	2	166	–	[24]
3CFM (2008)	1.60	0.192	2	282	–	[25]
3CBR (2008)	1.70	0.225	2	254	–	[26]
3D7P (2008)	1.72	0.223	2	157	–	[26]
2ROX (1996)	2.00	0.170	2	131	3,5,3',5'-Tetraiodo-L-thyronine	[3]
1TZ8 (2004)	1.85	0.198	4	322	Diethylstilbestrol	[27]

[a] The structure (1F41) is taken as template.

2.1. Identification of conserved water molecules and their mobility calculation

Conserved water molecules present in the apo transthyretin X-ray crystal structures (Table 1) were identified by standard least-square fitting algorithm in Swiss PDB Viewer program, where 1F41 PDB-structure was taken as template structure and the other structures (apo-protein) were superposed on its backbone. The Cα RMSD values were within ~0.2–0.8 Å. Conserved water molecular sites were identified by comparing the positions of the water molecules (oxygen atoms) which were found within 1.5 Å [30–32] between the superimposed template and reference structures. Mobility of the *i*-th water molecule of a crystal was calculated using respective B-factor and occupancy values following the formula [31,32]:

Mobility $M_i = (\mathrm{Bi}/\langle \mathrm{Bi} \rangle)/(O_i/\langle O_i \rangle)$, where B_i represents the B-factor for oxygen atom of the *i*-th crystal water molecule, and <Bi> denotes average B-factor for all water molecules present in respective X-ray structures. O_i indicates occupancy for *i*-th water molecule and $\langle O_i \rangle$ is the average occupancy of all water molecules present in the structure.

2.2. Molecular dynamics (MD) simulation

Molecular dynamics simulation of all the structures was performed using NAMD v.2.6 [33] with CHARMM27 force field [34,35]. Necessary topology and parameter files for thyroxin (T4) molecule and other ligands (Mod1-4, tafamidis, diflunisal and diclofenac) were generated by SwissParam program [36]. Then each structure was converted to Protein Structure File (PSF) by Automatic PSF Generation Plug-in within VMD program v. 1.8.6 [37]. Structures were solvated explicitly with TIP3P water model by retaining the crystal water molecules [38]. Cuboid water boxes were constructed around the protein (5 Å boundaries and 6–8 Å padding with approximately 5000 water molecules) using 'Solvate' program of VMD. Subsequent energy minimization was performed by conjugate gradient method. The process was conducted in three successive stages; firstly solvent water molecules for 2000 cycles, followed by crystal water molecules and the ligand (where present) along with solvent water molecules and finally the entire system, each for 1000 cycles. Then the energy minimized structures were simulated at constant temperature (300 K) and constant pressure (1 atm) by Langevin dynamics [39] using periodic boundary condition. Initially, 2 ns molecular dynamics (with time step 1 fs) was carried out for the equilibration of each system. In order to analyze the dynamic stability of that conserved water molecule [23–26] water dynamics was performed for 2 ns by fixing the ligand and protein residues, allowing the water molecules to move freely [40,41]. Then all atom molecular dynamics simulation for 5 ns was carried out on the equilibrated apo (1F41, 2QGB, 3CFM, 3CBR, 3D7P) and holo (2ROX) protein structures.

2.3. Ligand modification and molecular property study

Positional invariance of a water molecule with the 5′-iodine atom of 3,3′,5,5′-tetraiodo-L-thyronine (in X-ray and simulated structures) inspired us for covalent modification of the iodine atom (of the ligand) with more hydrophilic groups [e.g., amide ($CONH_2$), acetyl ($COCH_3$)] using HyperChem program [42]. Geometric optimization (steepest descent method) was carried out (using CHARMM force field) until the structure reached the convergence gradient 0.001 kcal/mole. OSIRIS Property Explorer [43] was used for toxicological test of the modified ligands and the existing drug tafamidis, diflunisal and diclofenac molecules. It is mainly based on RTECS (Registry of Toxic Effects of Chemical Substances) database, for predicting various undesirable effects (e.g., mutagenicity, tumorigenicity, irritation and reproductive) on human body. Properties with high risks of undesired effects are shown in red, whereas green color indicates drug conform behavior. Molecular properties like lipophilicity, number of donor–acceptor atoms, polar surface area (PSA), etc. were calculated using Molinspiration program [44].

2.4. Protein–ligand docking using AutoDock Vina

Biologically active tetrameric structure of hTTR has two ligand (T4) binding sites: one is flanked between the A- and C-chains and other between the B- and D-chains. Ligand–receptor docking study was separately performed (in both the ligand binding sites) using Autodock Vina v.1.1.1 [45]. The 1TZ8 X-ray structure [27] (excluding water and ligand molecules) was considered as receptor. Required PDBQT file of the receptor protein was generated using AutoDock Tools v.1.5.4 [46] by assigning Kollman united atom charges [47]. The structures for ligands and existing drug molecules (tafamidis, diflunisal and diclofenac) were converted into PDBQT file after including their partial atomic charges using Gasteiger method [48]. Grid point spacing was set at 1 Å and 20 grid points were taken in each direction. As the location of ligands inside the protein was already known, so grid box was centered at the ligand binding site. Vina automatically calculated the grid map for searching. All other docking parameters were assigned to their default values. We took the five best results (of docked complexes) according to their binding affinity.

2.5. Molecular dynamics simulation of the protein with modified ligands

To find out the actual impact of ligand modification (based on the protein ligand interaction) and to test the aquation potentiality of modified ligands (in bound condition), we performed MD-simulation of the docked complexes (Mod3 and Mod4 to tetrameric protein). Similar docking and simulation studies were also carried out with hTTR-T4 and hTTR-drug (tafamidis, diflunisal and diclofenac) complexes. Out of the five allowed conformations generated through docking, we took only one for each ligand, which ranked best in the energy series. Topology and parameter files were

Table 2
The H-bonding distances (Å), angles (subtended at W), B-factor and mobility of the invariant water molecule in different unliganded transthyretin crystal and energy minimized (*E*-min) structures.

PDB code	Invariant water (W) molecules PDB ID	B-factor/mobility	W···$S_{117}{}^{OG}$		W···$S_{117}{}^{OB}$		W···$T_{119}{}^{OG}$		S^{OG}_{117}···W···T^{OG}_{119}	
			Cryst	*E*-min	Cryst	*E*-min	Cryst	*E*-min	Cryst	*E*-min
1F41	36	27.00/0.76	2.74	2.91	3.02	4.08	2.74	2.84	112	106
2QGB	166	23.04/0.81	3.10	2.80	3.52	3.64	2.91	2.72	97	101
3CFM	135	17.97/0.52	2.98	2.87	3.39	3.81	3.04	2.83	112	106
3CBR	132	17.71/0.47	2.82	2.79	3.42	3.09	2.75	3.50	115	105
3D7P	136	26.31/0.64	2.82	2.85	3.42	3.75	2.71	3.22	119	98
Avg	–	22.41/0.64	2.89	2.84	3.35	3.67	2.83	3.02	111	103

generated for ligands. Then the complex structures were immersed in cuboid water boxes and energy minimization was carried. MD-simulation was followed for 2 ns with each structure (timestep 1 fs) applying CHARMM27 force-field using NAMD v.2.6.

3. Results and discussion

Detail analyses of the X-ray crystal structures of unliganded TTR have revealed the presence of a conserved hydrophilic center (occupied by one water molecule, W36 in 1F41, W166 in 2QGB, W135 in 3CFM, W132 in 3CBR and W136 in 3D7P) which forms strong H-bonds with the side chain and backbone atoms of Ser117 and Thr119, two important residues of thyroxin binding pocket of protein [23]. Similar type of interaction is also observed in the energy minimized and MD simulated trajectories of those unliganded X-ray structures. Mobility and B-factor of the water molecule (Table 2) in all the TTR-structures indicate some functional importance of that hydrophilic center related to the thyroxin binding chemistry.

Careful investigation of the X-ray crystal structures of apo-transthyretin (1F41, 2QGB, 3CFM, 3CBR and 3D7P) reveal that the water molecule (W) forms strong H-bond with the side-chain oxygen (OG) of Ser117 and Thr119 with average distances 2.89 and 2.83 Å [23–26]. Angle made by the OG atoms of the respective residues at the water molecule is ∼110°. After energy minimization, the water molecule shifts slightly outward (from its initial position) resulting the increase in W···Ser117(OB) distance. However, H-bonds between the water molecule and Ser117(OG)/Thr119(OG) are retained. Subsequently, with a view to confirm the importance of that water molecule, it was removed from all the structures and energy minimization was followed on the solvated structures (keeping the other water molecules intact). One water molecule appeared in that invariant hydrophilic position and formed similar types of H-bond interaction with Ser117 and Thr119. However, no such water molecule was observed in that invariant hydrophilic position of the ligand-bound transthyretin X-ray or energy minimized structures of 2ROX. After superimposition of the structures, position of the 5′-I (iodine) atom of thyroxin in holo-TTR and the invariant water molecule in apo-TTR are observed to be approximately same. All the above facts suggest that the conserved water molecule may play some significant role in TTR–thyroxin complexation.

During water dynamics of solvated apo-TTR X-ray structures, the water bridge Ser117(OG)···W···Thr119(OG) remains intact throughout the simulation trajectories. The W···Ser117(OG) distance varies within 2.66–3.17 Å except in 2QGB and 3CFM structures, where the water molecule moves a little away for some period (∼500–550 and ∼1400–1650 ps in 2QGB and ∼700–900 ps in 3CFM); however, after some time strong H-bond interaction is recovered. In all these structures, W···Thr119(OG) H-bond interaction is observed (2.4–3.5 Å) throughout the trajectories except for a very short period in 3CBR (Table 3). During MD simulation, increase in W···Ser117(OB) mean distance is observed in different structures, which is reflected in variation of average residential frequencies of the H-bond interaction (30, 10, 15 and 25%) in 1F41, 2QGB, 3CFM and 3D7P structures, whereas it appears 95% in 3CBR. In all the structures angle subtended at W by Ser117(OG) and Thr119(OG) changes between ∼95° and 110° except in 3CBR where it increases to 115° for a short span of time (∼200 ps).

Some conformational changes in the side chain orientation of Ser117 are observed during MD-simulation of all the apo-protein structures (1F41, 2QGB, 3CFM, 3CBR and 3D7P), which is clearly reflected in the variation of chi-1 (χ1) angle of that residue (Fig. 2A). Due to this conformational flexibility, sometime the W···Ser117 interaction disappears and the residue is stabilized by other water molecule (W′). The minor variation of chi-1 (χ1) angle in Thr119 indicates its lower flexibility (Fig. 2B) compared to Ser117, which might be effective for holding that conserved water molecule. But when we compare MD-simulation trajectory of the ligand bound structure (2ROX), it clearly shows that Thr119 adopts a new orientation and is stabilized by Ala120(OB) through direct or water mediated (W″) H-bond interaction (Fig. 3), however, the flexibility of Ser117 side chain is much restricted in ligand-bound structure compared to apo form.

So the simulation results of several unliganded and ligand-bound TTR structures indicate an important role of that conserved hydrophilic center in protein–T4 complexation. In unliganded TTR, mouth of the innermost ligand binding pocket remains closed by this conserved water center, which bridges Ser117(OG) and Thr119(OG) through H-bonds. In protein–T4 complex, T4 molecule replaces that conserved water molecule. During the migration of that water molecule, the side chains of Ser117 and Thr119 adopt anti-conformation, which stereo-chemically assist the thyroxin molecule to occupy its specific binding site (Fig. 4). So, the mobility of that water molecule as well as the flexibility of Ser117/Thr119 side chains and Ser···W···Thr119 water bridge may be involved either in the function of TTR or in the self-aggregation of monomers. The aggregation mechanism of TTR into amyloid fibrils involves a multistep self-assembly process, the TTR tetramer first dissociates into native monomer, then unfolding or changes in monomeric conformations, followed by the aggregation of conformationally modified monomers into non-fibrillar oligomers that latter form proto-fibrils and further elongate into mature fibrils [49–51]. The amyloid inhibitors appear to function by shifting the aggregation equilibrium away from the amyloid state by increasing the kinetic barrier associated with misfolding, preventing amyloidogenesis by stabilizing the native state [16]. But those studies could not reflect any clear idea on the role of that water bridge (Ser117···W···Thr119) or on the mobility of that water molecule to aggregation process. In context to the aggregation behavior of TTR, several biochemical and X-ray studies have been made. Currently 80 single point mutations on TTR are known [52]. Among these single point mutations, only one shows a nondisease effect and that is Thr119Met [17] Moreover, the X-ray structure of mutated (Thr119Met) unliganded TTR (1FHN) [53], where two TTR molecules are associated as dimer in the asymmetric unit of the crystal, shows the absence of water molecule in

Table 3
Water (W) mediated H-bonding distances (Å) and angles (subtended at W) during 2 ns water dynamics simulation of different unliganded solvated TTR structures.

Interaction	PDB code	1F41	2QGB	3CFM	3CBR	3D7P
$S_{117}{}^{OG}\cdots W$	Avg	2.96	3.14	3.07	2.83	2.83
	Min	2.75	2.72	2.70	2.66	2.74
	Max	3.17	3.78	3.90	3.04	2.94
	Std. dev.	0.17	0.49	0.54	0.15	0.08
	Frqn[a]	100	85	80	100	100
$S_{117}{}^{OB}\cdots W$	Avg	3.81	3.97	3.83	3.35	3.76
	Min	3.45	3.54	3.55	3.09	3.55
	Max	4.08	4.52	4.10	3.54	3.88
	Std. dev.	0.25	0.41	0.25	0.02	0.13
	Frqn[a]	30	10	15	95	25
$T_{119}{}^{OG}\cdots W$	Avg	2.89	3.03	2.93	3.45	3.21
	Min	2.84	2.72	2.83	3.21	3.02
	Max	2.98	3.32	3.05	3.60	3.47
	Std. dev.	0.06	0.24	0.10	0.17	0.19
	Frqn[a]	100	100	100	95	100
$S_{117}^{OG}\cdots W\cdots T_{119}^{OG}$	Avg	104	98	108	108	98
	Min	98	95	100	103	95
	Max	111	101	115	115	103
	Std. dev.	5	2	6	5	3

[a] Refers to the Residential frequency of the H-bond interaction.

that conserved hydrophilic position attached to Ser117 and Thr119. In most of the TTR crystal structures *B*-values (temperature factor) of Ser117/Thr119 bound water molecules vary from 15 to 28 $Å^2$, reflecting their high mobilities within the conformationally unchanged protein structure. So, it can be speculated that the water molecule or Ser117···W···Thr119 water bridge may not play any significant role in the self-aggregation of TTR which causes amyloid disease. After investigating the topological consequences of T4 binding chemistry and geometrical features of the conserved water molecular interaction (during dynamics) with Ser117 and Thr119 sites, we are interested to design a few T4 analogs by modifying the 5′ or 3′ or both the iodine atoms of thyroxin using conserved water mimic inhibitor design protocol.

Subsequently, attempt has been made for covalent modification of the 5′-iodine atom of thyroxin (Fig. 5A) with more hydrophilic amide (—$CONH_2$) group. The modified ligand Mod1 (Fig. 5B) is separately docked in both the thyroxin binding cavities (flanged by A–C and B–D chains) of tetrameric protein 1TZ8 PDB-structure. For comparative study, similar type of docking is performed with T4 in the 1TZ8 structure. The modified ligand seems to bind better

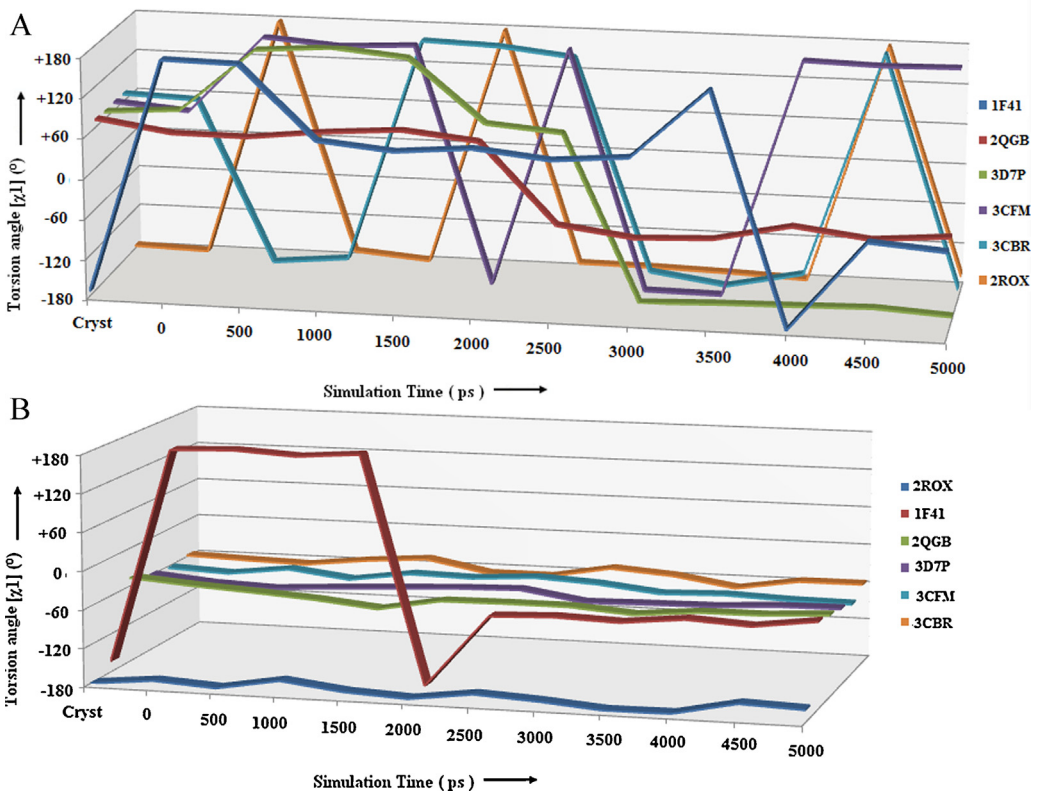

Fig. 2. (A) Torsion angles ($\chi 1$) of Ser117 side chain of apo-tarnsthyretin (1F41, 2QGB, 3CFM, 3CBR and 3D7P) and holo-transthyretin (2ROX) structures during their MD simulation. (B) Torsion angles ($\chi 1$) of Thr119 side chain of apo-tarnsthyretin (1F41, 2QGB, 3CFM, 3CBR and 3D7P) and holo-transthyretin (2ROX) structures during their MD simulation.

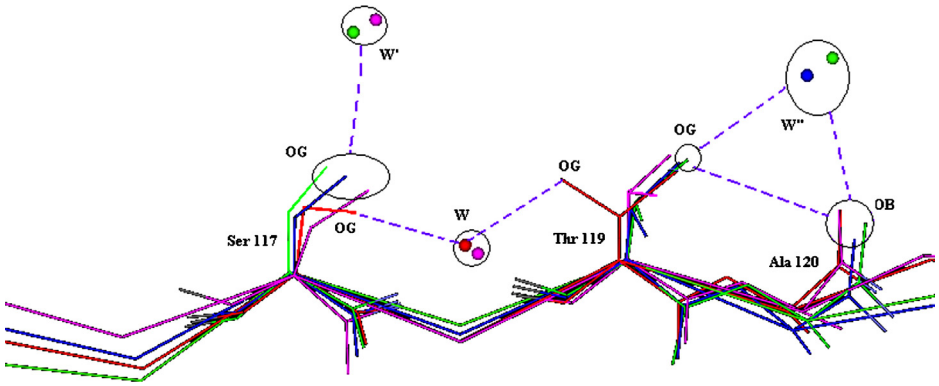

Fig. 3. Superposition of Ser117 and Thr119 residues of the X-ray crystal structures of 1F41 (red), 2ROX (blue) and their MD-simulated structures (pink and green respectively) showing their side chain conformational change during ligand binding and water mediated stabilization.

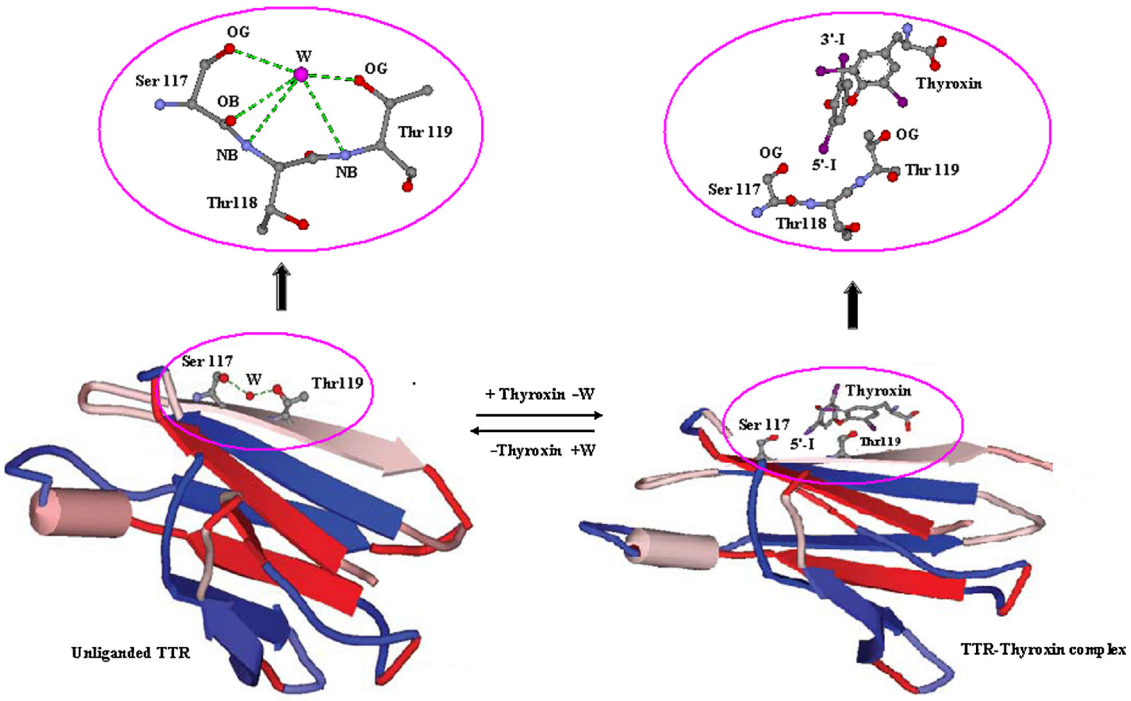

Fig. 4. Transition from unliganded to liganded bound conformation of TTR. Thyroxin molecule (T4) replaces one conserved water molecule (W) and side chains of the respective Ser117 and Thr119 adopt a trans-like conformation.

Table 4
Binding energy (KJ/mole) for the natural ligand (Thyroxin), existing drugs [Tafamidis (Taf), Diflunisal (Dif)and Diclofenac (Dic)] and all the modified ligands (Mod1–4), within the ligand binding pockets flanged between the A–C and B–D chains.

Conformations	1TZ8(A–C chains)							
	T4	Mod1	Mod2	Mod3	Mod4	Taf	Dif	Dic
1	−6.6	−7.1	−7.6	−8.4	−8.6	−7.9	−7.7	−7.4
2	−6.5	−7.0	−7.5	−8.3	−8.6	−7.9	−7.6	−7.3
3	−6.5	−7.0	−7.4	−8.2	−8.5	−7.9	−7.1	−7.3
4	−6.5	−6.9	−7.4	−8.2	−8.4	−7.9	−7.0	−7.0
5	−6.5	−6.9	−7.3	−8.1	−8.4	−7.9	−6.8	−7.0
Conformations	1TZ8(B–D chains)							
	T4	Mod1	Mod2	Mod3	Mod4	Taf	Dif	Dic
1	−6.3	−6.7	−7.2	−7.8	−7.9	−7.5	−8.0	−7.3
2	−6.2	−6.7	−7.1	−7.8	−7.8	−7.5	−7.6	−7.2
3	−6.1	−6.7	−6.9	−7.8	−7.7	−7.4	−7.6	−7.1
4	−6.0	−6.6	−6.8	−7.8	−7.7	−7.3	−7.4	−7.1
5	−6.0	−6.5	−6.8	−7.7	−7.7	−7.3	−7.3	−7.0

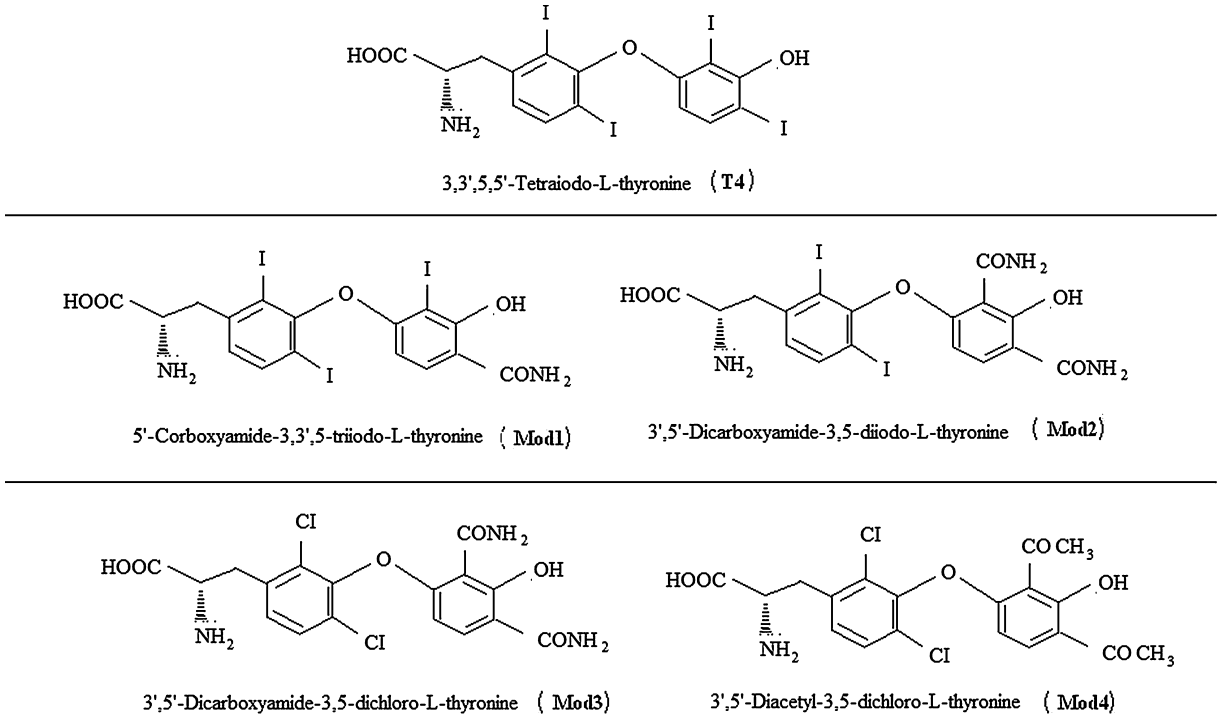

Fig. 5. Schematic presentation of Thyroxin molecule and its structural (modified) analogs. (A) 3,3′,5,5′-Tetraiodo-L-thyronine (T4). (B) 5′-Carboxyamide-3,3′,5-triiodo-L-thyronine (Mod1). (C) 3′,5′-Dicarboxyamide-3,5-diiodo-L-thyronine (Mod2). (D) 3′,5′-Dicarboxyamide-3,5-dichloro-L-thyronine (Mod3). (E) 3′,5′-Diacetyl-3,5-dichloro-L-thyronine (Mod4).

(binding energy −7.1 and −6.7 kJ/mole for the pockets within A–C and B–D chains) compared to thyroxin (−6.6 and −6.3 kJ/mole) (Table 4). Again, the 3′-iodine atom (which exhibits similar type of interaction with the other chain of ligand binding cavity) is replaced with amide (—$CONH_2$) group. Further docking studies have shown the increasing trend of binding energy (−7.6 and −7.2 kJ/mole) for modified ligand Mod2 (Fig. 5C).

Molecular properties and toxicity risk assessment of Mod1 and Mod2 (using Molinspiration and OSIRIS Property Explorer) were found to be free from the risk of undesired effects ilke mutagenicity or tumorigenicity (Table 5). They are nonirritant and have no adverse effect on reproductivity. The *C* log *P* value for both the ligands seem to be much lower (3.10 and 1.15 respectively) compared to T4 (5.03). Drug scores of the modified ligands are also better (0.15 and 0.2) than T4 (0.1). However, Mod1 and Mod2 do not conform to Lipinski's rule of 5 [54] in two points, molecular mass (694 and 611) and number of hydrogen-donor atoms (6 and 8). The TPSA (total polar surface area) and volume of Mod2 is slightly higher (178.97 $Å^2$ and 352.9 $Å^3$) compared to natural ligand T4 (92.78 $Å^2$ and 340.33 $Å^3$). To reduce the molecular mass and volume of Mod2, we have replaced both the iodine atoms at 3 and 5 positions by chlorine atoms and modeled Mod3. Further docking of Mod3 (Fig. 5D) at both the ligand binding cavities of protein, the binding energy values change to −8.4 and −7.8 kJ/mole. Drug score of the modified ligand increases to 0.31 and *C* log *P* value goes down to 0.51. Molecular mass and volume is found to be 427 and 332 $Å^3$. Now, confrontation with Lipinski's rule reduces to one (i.e., the number of hydrogen-donor atoms), but TPSA value remains a little higher.

In order to decrease the polar surface area and number of hydrogen-donor atoms, substitution with acetyl (—$COCH_3$) group at the 3′ and 5′ positions of Mod3 have been made, retaining the chlorine atoms at 3 and 5 positions. This modified ligand Mod4 (Fig. 5E) has molecular mass 426.25 (almost same as Mod3) and volume 342.5 $Å^3$ with number of hydrogen-donor atom 4, which are close or equal to the natural ligand T4. TPSA value (126.9 $Å^2$) is well below the cut off line. The *C* log *P* value and drug score are 2.3 and

Table 5
Molecular properties and Toxicological Risk Assessment data of Thyroxin, existing drugs [Tafamidis (Taf), Diflunisal (Dif) and Diclofenac (Dic)] and the modified ligands (Mod1–4).

	T4	Mod1	Mod2	Mod3	Mod4	Taf	Dif	Dic
C log P	5.03	3.1	1.15	0.51	2.3	4.38	3.0	4.4
Mol. wt.	776.87	694	611.13	427	426.25	307	250	296
Drug score	0.1	0.15	0.2	0.31	0.25	0.2	0.15	0.36
n OH-NH	4	6	8	8	4	1	2	2
TPSA	92.78	135.88	178.97	178.97	126.93	63.33	57.5	49.32
n Rotatable Bond	5	6	7	7	7	2	2	4
n Atom	24	26	28	28	28	20	18	19
Volume	340.33	346.6	352.9	331.9	342.5	230.9	200.33	238.73
n Violation	1	2	2	1	0	0	0	0
Mutagenic	Green	Green	Green	Green	Green	Yellow	Red	Green
Tumorigenic	Green	Green	Green	Green	Green	Green	Green	Green
Irritant	Green	Green	Green	Green	Green	Green	Green	Green
Reproductive	Green	Green	Green	Green	Green	Green	Red	Red

Red indicates properties with high risk of undesired effects like mutagenicity or poor intestinal absorption whereas Green color indicates drug conform behavior.

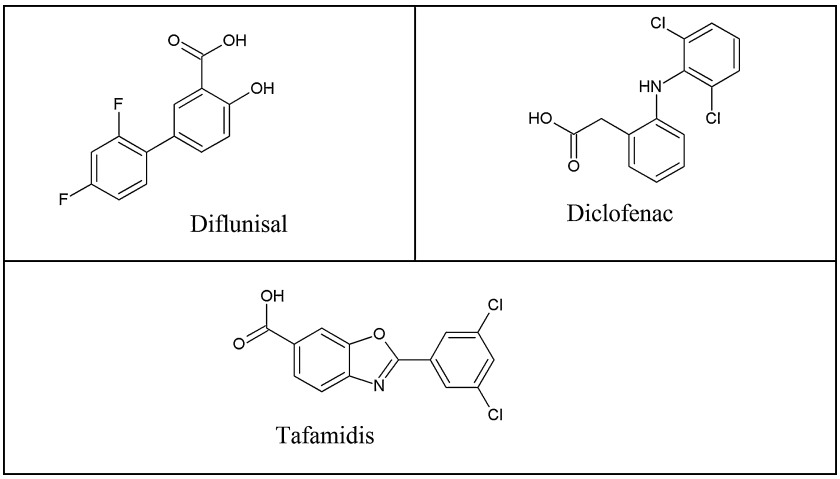

Fig. 6. The chemical structures of Diflunisal, Diclofenac and Tafamidis.

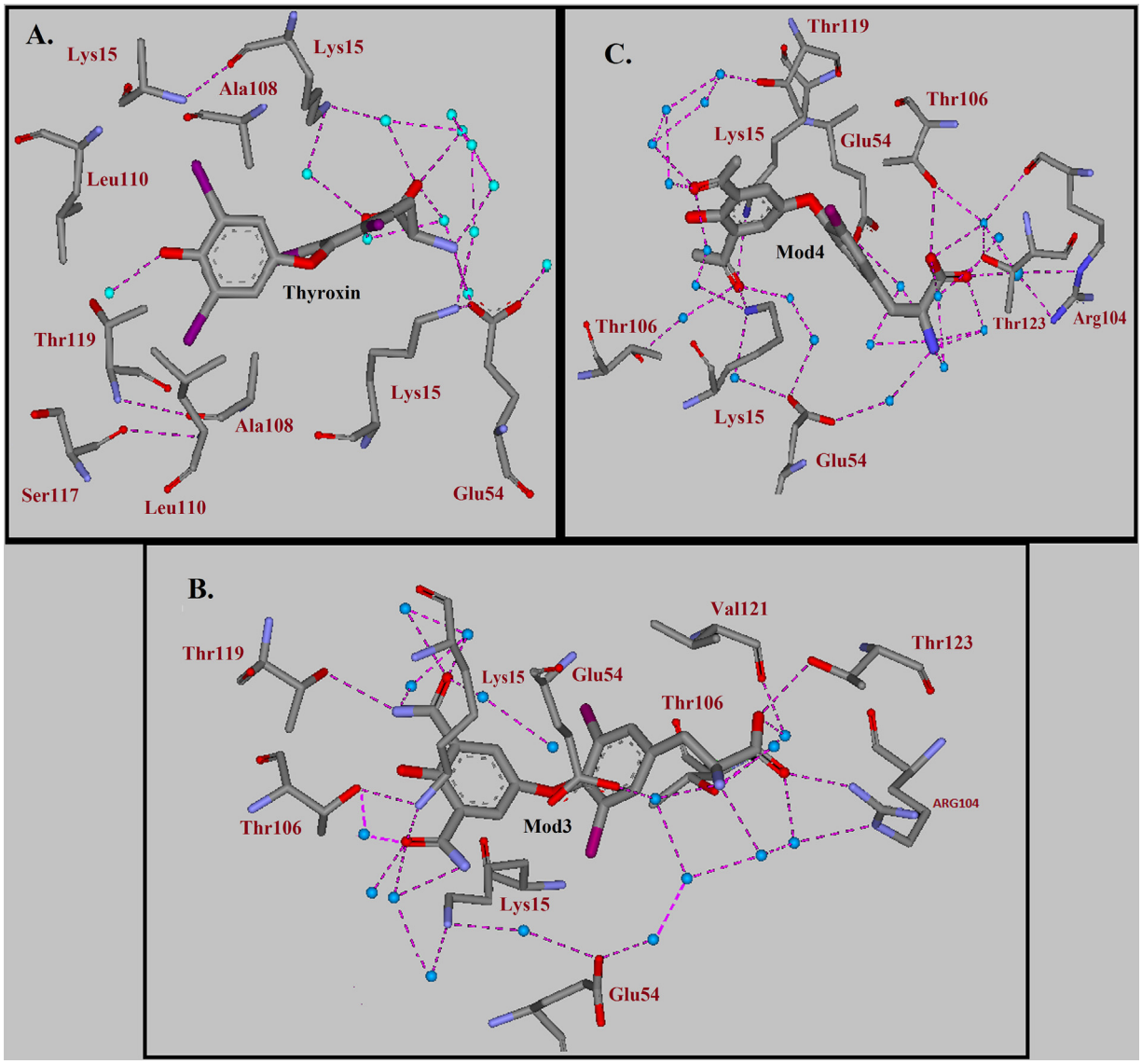

Fig. 7. Stabilization and hydration susceptibility of thyroxin and its modified analogs in (A) hTTR – T4 complex, (B) hTTR – Mod3 complex, (C) hTTR – Mod4 complex.

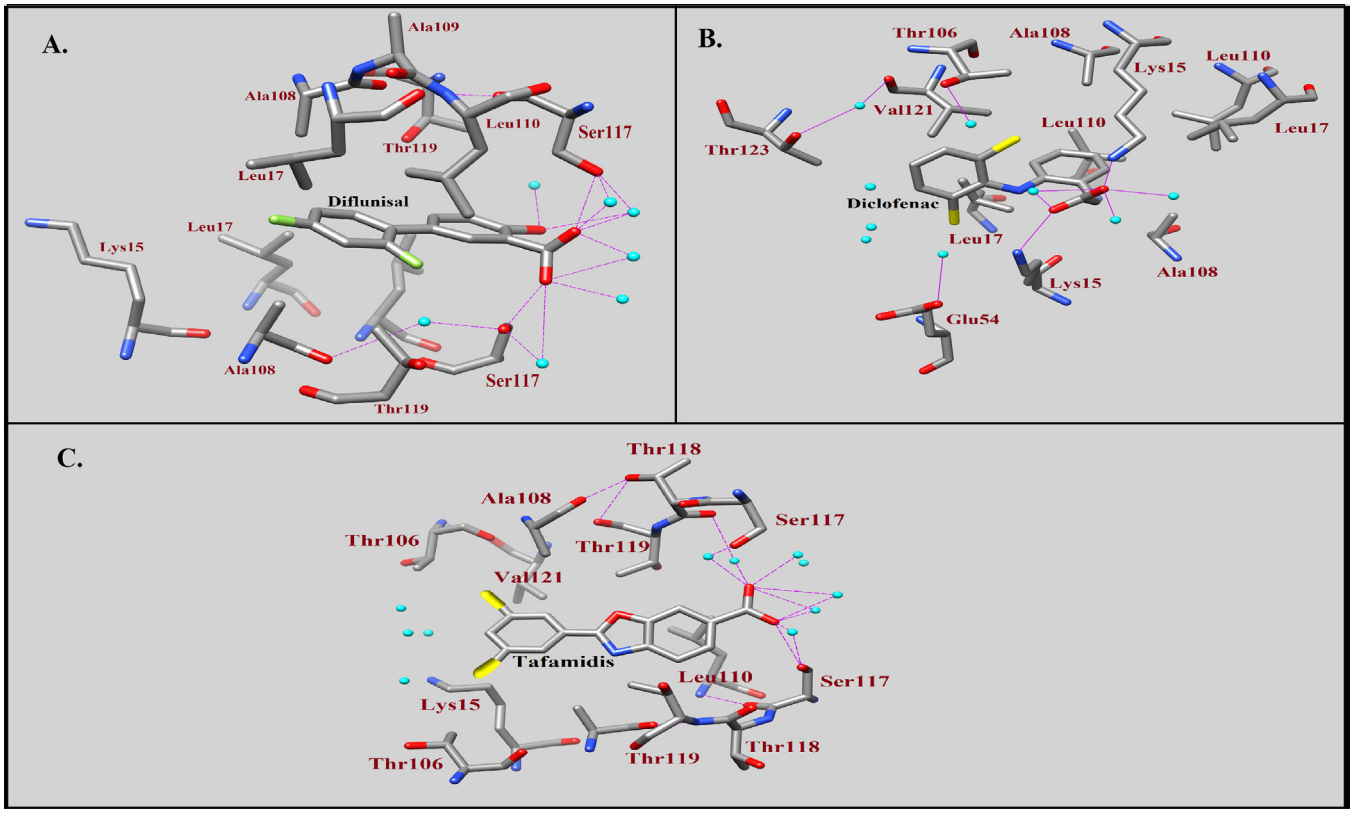

Fig. 8. The interaction of drug molecules with hTTR after 2ns MD-Simulation: (A) hTTR – Diflunisal complex, (B) hTTR – Diclofenac complex, (C) hTTR-Tafamidis complex.

0.25. During docking of Mod4 to the respective cavities of A–C and B–D chains of the protein, binding energy values increase to −8.6 and −7.9 kJ/mole (Table 4). During the analysis of binding energy data for all the (modified and natural) ligands one interesting fact appears, that the pocket flanged between the A–C chains shows a greater affinity toward the ligand compared to the B–D chains. It was previously reported by Wojtczak et al. [4] and they described it as allosteric effect. Interestingly when we docked the molecules (T4 or its analogs) separately in those cavities, the binding energy values were observed to be different, which might occur due to some conformational differences of the amino acid residues of those two ligand binding pockets. For getting an idea on the interaction of the existing drug molecules (whose chemical structures are shown in Fig. 6) with TTR we have also docked tafamidis, diflunisal and diclofenac to ligand binding pockets flanged by the A–C and the B–D chains.The binding energy values are −7.9 and −7.5 kJ/mole for tafamidis, −8.0 and −7.7 kJ/mole for diflunisal and −7.4 and −7.3 kJ/mol for diclofenac, and the values are included in Table 4. These energy values are comparatively lower than Mod3 and Mod4 in their protein complexes. The molecular/pharmacological properties of drugs tafamidis, diflunisal and diclofenac are included in Table 5. The properties of Mod4 seem to be comparable to those drug molecules; it even shows better values for drug score, etc.

MD simulation studies of the docked complexes of Mod3, Mod4 and T4 with the protein reveal some interesting features about their structural stability. No covalent or H-bond interaction is observed between the ligand and the protein in the T4-protein docked complex (Fig. 7A), which seems quite similar to X-ray crystallographic structure of 2ROX. In the MD simulation study of T4-protein docked complex, one water molecule (residential frequency 95%) appears to form H-bond with the phenolic-OH group of T4, though it is missing in the X-ray structure. However, in the MD simulation trajectory of 2ROX X-ray structure that conserved water molecule appears with residential frequency of 80%. In dynamic structures of protein–ligand complexes, both Mod3 and Mod4 are stabilized by a water network through the interaction with Glu54(OD). Nitrogen atom of carboxyamide group of Mod3 is stabilized by the side chains of Lys15, Thr106 and Thr119 (polar amino acid residues) through direct or water mediated H-bond interaction. In Mod3–protein complex, Lys15(NZ) stabilizes the CO group (at 5′ position) by direct H-bonding interaction, whereas Thr106(OG) stabilizes it through water mediated H-bond (Fig. 7B). The carboxyamide nitrogen atom (at 3′ position) is stabilized by Thr119(OG). During dynamics similar type of interaction has also been observed in Mod4–protein docked complex. The oxygen atom of acetyl group (5′ position) is stabilized through direct H-bond interaction with Lys15(NZ) and Thr106(OG). The acetyl CO (at 3′ position) is stabilized by a water network anchored through Thr119(OG) (Fig. 7C). The increasing trends of hydration susceptibility for Mod3 and Mod4 have also been revealed in the MD-simulated structures of their docked complexes. In the 2 ns MD-simulated protein–drug complex structures, carboxylic acid groups of both the tafamidis and diflunisal are stabilized by Ser117 (of both the chains of protein) through direct as well as water mediated H-bonds. The carboxylic acid group of diclofenac is stabilized by Lys15 of both the chains of the protein through direct H-bonds. The interaction of diflunisal, diclofenac and tafamidis with hTTR in the simulated structures is shown in Fig. 8. These three drug molecules have not shown any other type of polar interaction with TTR. However they may be stabilized by hydrophobic interaction.

4. Conclusion

Simulation studies of human apo-transthyretin X-ray structures have supported the importance of a conserved water molecule in the stabilization of Ser117 and Thr119 residues in unliganded protein. Migration of a conserved water molecule from the hydrophilic center may induce conformational changes in Ser117 and Thr119

residues which could favor the binding of thyroxin molecule (or its analogs) in the inner core of ligand binding site. Interactive binding features of that conserved water molecule at thyroxin (T4) binding site as well as the dynamics of Ser117 and Thr119 in unliganded and ligand-bound forms of TTR have been utilized for the design of four covalently modified T4 analogs (Mod1-4). Binding energies obtained from docking studies and theoretically investigated pharmacological parameters indicate the plausibility of these modeled compounds to act as inhibitors for TTR associated amyloid diseases, among them Mod4 (3′,5′-diacetyl-3,5-dichloro-L-thyronine) may thought to be the best in the series.

Acknowledgement

A.B and B.P.M acknowledge the National Institute of Technology (Govt. of India) – Durgapur for providing research facilities at the Department of Chemistry.

References

[1] L. Bartalena, J. Robbins, Thyroid hormone transport proteins, Clinics in Laboratory Medicine 13 (1993) 583–598.
[2] C.C. Blake, M.J. Geisow, S.J. Oatley, B. Rerat, C. Rerat, Structure of prealbumin: secondary, tertiary and quaternary interactions determined by Fourier refinement at 1.8, Journal of Molecular Biology 121 (1978) 339–356.
[3] A. Wojtczak, V. Cody, J.R. Luft, W. Pangborn, Structures of human transthyretin complexed with thyroxine at 2.0 Å resolution and 3′,5′-dinitro-Nacetyl-L-thyronine at 2.2 Å resolution, Acta Crystallographica Section D: Biological Crystallography 52 (1996) 758–765.
[4] S.F. Nilsson, L. Rask, P.A. Peterson, Studies on thyroid hormone-binding proteins. II. Binding of thyroid hormones, retinol-binding protein, and fluorescent probes to prealbumin and effects of thyroxine on prealbumin subunit self association, Journal of Biological Chemistry 250 (1975) 8554–8563.
[5] J.A. Hamilton, M.D. Benson, Transthyretin: a review from a structural perspective, Cellular and Molecular Life Sciences 58 (2001) 1491–1521.
[6] E. Ciszak, V. Cody, J.R. Luft, Crystal structure determination at 2.3-Å resolution of human transthyretin-3′,5′-dibromo-2′,4,4′,6-tetrahydroxyaurone complex, Proceedings of the National Academy of Sciences of the United States of America 89 (1992) 6644–6648.
[7] V. Cody, Mechanisms of molecular recognition: crystal structure analysis of human and rat transthyretin inhibitor complexes, Clinical Chemistry and Laboratory Medicine 40 (2002) 1237–1243.
[8] L. Lin, R.M. Murphy, Kinetics of inhibition of β-amyloid aggregation by transthyretin, Biochemistry 45 (2006) 15702–15709.
[9] J.W. Kelly, Amyloid fibril formation and protein misassembly: a structural quest for insights into amyloid and prion diseases, Structure 5 (1997) 595–600.
[10] G.G. Cornwell 3rd, K. Sletten, B. Johansson, P. Westermark, Evidence that the amyloid fibril protein in senile systemic amyloidosis is derived from normal prealbumin, Biochemical and Biophysical Research Communications 154 (1988) 648–653.
[11] P. Westermark, K. Sletten, B. Johansson, G.G. Cornwell 3rd, Fibril in senile systemic amyloidosis is derived from normal transthyretin, Proceedings of the National Academy of Sciences of the United States of America 87 (1990) 2843–2845.
[12] M.J. Saraiva, Transthyretin mutations in health and disease, Human Mutation 5 (1995) 191–196.
[13] P. Gambetti, C. Russo, Human brain amyloidoses, Nephrology Dialysis Transplantation 13 (1998) 33–40.
[14] Y. Sekijima, R.L. Wiseman, J. Matteson, P. Hammarstrom, S.R. Miller, The biological and chemical basis for tissue-selective amyloid disease, Cell 121 (2005) 73–85.
[15] J.N. Buxbaum, C.E. Tagoe, The genetics of the amyloidoses, Annual Review of Medicine 51 (2000) 543–569.
[16] P. Hammarstrom, R.L. Wiseman, E.T. Powers, J.W. Kelly, Prevention of transthyretin amyloid disease by changing protein misfolding energetic, Science 299 (2003) 713–716.
[17] P. Hammarstrom, F. Schneider, J.W. Kelly, Trans-suppression of misfolding in an amyloid disease, Science 293 (2001) 2459–2461.
[18] J.C. Sacchettini, J.W. Kelly, Therapeutic strategies for human amyloid diseases, Nature Reviews Drug Discovery 1 (2002) 267.
[19] S. Connelly, J.W. Kelly, I.A. Wilson, Tafamidis, a potent and selective transthyretin kinetic stabilizer that inhibits the amyloid cascade, Proceedings of the National Academy of Sciences of the United States of America 109 (2012) 9629–9634.
[20] M.G. McCammon, D.J. Scott, C.A. Keetch, L.H. Greene, H.E. Purkey, Screening transthyretin amyloid fibril inhibitors: characterization of novel multiprotein, multiligand complexes by mass spectrometry, Structure 10 (2002) 851–863.
[21] L. Bartalena, A. Pinchera, Effects of thyroxin excess on peripheral organs, Acta Medica Austriaca 21 (1994) 60–65.
[22] T. Klabunde, H.M. Petrassi, B. Vibha, V.B. Oza, P. Raman, J.W. Kelly, J.C. and, Sacchettini, Rational design of potent human transthyretin amyloid disease inhibitors, Nature Structural & Molecular Biology 7 (2000) 312–321.
[23] A. Hörnberg, T. Eneqvist, A. Olofsson, E. Lundgren, A.E. Sauer-Eriksson, A comparative analysis of 23 structures of the amyloidogenic protein transthyretin, Journal of Molecular Biology 02 (2000) 649–669.
[24] S.M. Johnson, S. Connelly, I.A. Wilson, J.W. Kelly, Biochemical and structural evaluation of highly selective 2-arylbenzoxazole-based transthyretin amyloidogenesis inhibitors, Journal of Medicinal Chemistry 51 (2008) 260–270.
[25] L.M. Lima, V.D. Silva, L.D. Palmieri, M.C. Oliveira, D. Foguel, I. Polikarpov, Identification of a novel ligand binding motif in the transthyretin channel, Bioorganic & Medicinal Chemistry 18 (2010) 100–110.
[26] S.K. Palaninathan, N.N. Mohamedmohaideen, W.C. Snee, J.W. Kelly, J.C. Sacchettini, Structural insight into pH induced conformational changes within the native human transthyretin tetramer, Journal of Molecular Biology 382 (2008) 1157–1167.
[27] E. Morais-de-Sá, P.J. Pereira, M.J. Saraiva, A.M. Damas, The crystal structure of transthyretin in complex with diethylstilbestrol: a promising template for the design of amyloid inhibitors, Journal of Molecular Biology 279 (2004) 53483–53490.
[28] H.M. Berman, J. Westbrook, Z. Feng, G. Gilliand, T.N. Bhat, H. Weissig, I.N. Shindyalov, P.E. Bourne, The Protein Data Bank, Nucleic Acids Research 28 (2000) 235–242.
[29] N. Guex, A. Diemand, M.C. Peitsch, T. Schwede, The Deep View-The Swiss-Pdb View Programme, an Environment for Comparative Protein Modeling, Glaxo Smith Kline R&D, 2001.
[30] K. Ogata, S.J. Wodak, Conserved water molecules in MHC class-I molecules and their putative structural and functional roles, Protein Engineering 15 (2002) 697–705.
[31] G. Mustata, J.M. Briggs, Cluster analysis of water molecules in alanine racemase and their putative structural role, Protein Engineering, Design and Selection 17 (2004) 223–234.
[32] T.K. Nandi, H.R. Bairagya, B.P. Mukhopadhyay, K. Sekar, D. Sukul, A.K. Bera, Conserved water-mediated H-bonding dynamics of catalytic Asn 175 in plant thiol protease, Journal of Bioscience 34 (2009) 27–34.
[33] L. Kale, R. Skeel, M. Bhandarkar, R. Brunner, A. Gursoy, N. Krawetz, J. Phillips, A. Shinozaki, K. Varadarajan, K. Schulten, NAMD2: greater scalability for parallel molecular dynamics, Journal of Computational Physics 151 (1999) 283–312.
[34] B.R. Brooks, R.E. Bruccoleri, B.D. Olafson, D.J. States, S. Swaminathan, M. Karplus, CHARMM: a program for macromolecular energy, minimization, and dynamics calculations, Journal of Computational Chemistry 4 (1983) 187–217.
[35] A.D. MacKerell Jr., D. Bashford, et al., All-atom empirical potential for molecular modeling and dynamics studies of proteins, Journal of Physical Chemistry B 102 (1998) 3586–3616.
[36] V. Zoete, M.A. Cuendet, A. Grosdidier, O. Michielin, SwissParam, a fast force field generation tool for small organic molecules, Journal of Computational Chemistry 32 (2011) 2359–2368.
[37] W. Humphrey, A. Dalke, K. Schulten, Vmd – visual molecular dynamics, Journal of Molecular Graphics 14 (1996) 33–38.
[38] J.H. Welsh, Y. Lin, Discussion of the catalytic pathway of cysteine proteases AM 1 calculations, Journal of Molecular Structure: THEOCHEM 401 (1997) 315–326.
[39] J. Gullingsrud, D. Kosztin, K. Schulten, Structural determinants of MscL gating studied by molecular dynamics simulations, Biophysical Journal 80 (2001) 2074–2081.
[40] V. Leroux, N. Gresh, W.Q. Liu, C. Garbay, B. Maigret, Role of water molecules for binding inhibitors in the SH2 domain of Grb2: a molecular dynamics study, Journal of Theoretical Chemistry 806 (2007) 51–66.
[41] H.R. Bairagya, B.P. Mukhopadhyay, S. Bhattacharya, Role of the conserved water molecules in the binding of inhibitor to IMPDH-II (human): a study on the water mimic inhibitor design, Journal of Molecular Structure: THEOCHEM 908 (2009) 31–39.
[42] Hyperchem TM Release 7.52 for windows Molecular Modeling System Copyright_2005 Hypercube, Inc.
[43] E.L. Piparo, A. Worth, Review of QSAR Models and Software Tools for predicting Developmental and Reproductive Toxicity: JRC Scientific & Technological Report, 2010, http://dx.doi.org/10.2788/9628.
[44] P. Ertl, B. Rohde, P. Selzer, Fast calculation of molecular polar surface area as a sum of fragment-based contributions and its application to the prediction of drug transport properties, Journal of Medicinal Chemistry 43 (2000) 3714–3717.
[45] O. Trott, A.J. Olson, AutoDock Vina: improving the speed and accuracy of docking with a new scoring function, efficient optimization and multithreading, Journal of Computational Chemistry 31 (2010) 455–461.
[46] G.M. Morris, R. Huey, W. Lindstrom, M.F. Sanner, R.K. Belew, D.S. Goodsell, A. Olson, Automated docking with selective receptor flexibility, Journal of Computational Chemistry 30 (2009) 2785–2791.
[47] S.J. Weiner, P.A. Kollman, D.A. Case, U.C. Sing, C. Ghio, G. Alagona, S. Profeta, P. Weiner, A new force field for molecular mechanical simulation of nucleic acids and proteins, Journal of the American Chemical Society 106 (1984) 765–784.
[48] J. Gasteiger, M. Marsili, Iterative partial equalization of orbital electronegativity – a rapid access to atomic charges, Tetrahedron 36 (1980) 3219–3228.
[49] T.R. Foss, R.L. Wiseman, J.W. Kelly, The pathway by which the tetrameric protein transthyretin dissociates, Biochemistry 44 (2005) 15525–15533.
[50] A.R. Hurshman, J.T. White, E.T. Powers, J.W. Kelly, Transthyretin aggregation under partially denaturing conditions is a downhill polymerization, Biochemistry 43 (2004) 7365–7381.

[51] A. Quintas, D.C. Vaz, I. Cardoso, M.J.C. Saraiva, R.M.M. Brito, Tetramer dissociation and monomer partial unfolding precedes protofibril formation in amyloidogenic transthyretin variants, Journal of Biological Chemistry 276 (2001) 27207–27213.
[52] X. Jiang, J.N. Buxbaum, J.W. Kelly, The V122I cardiomyopathy variant of transthyretin increases the velocity of rate-limiting tetramer dissociation, resulting in accelerated amyloidosis, Proceedings of the National Academy of Sciences of the United States of America 98 (2001) 14943–14948.
[53] M.P. Sebastiao, V. Lamzin, M.J. Saraiva, A.M. Damas, Transthyretin stability as a key factor in amyloidogenesis: X-ray analysis at atomic resolution, Journal of Molecular Biology 306 (2001) 733–744.
[54] C.A. Lipinski, F. Lombardo, B.W. Dominy, P.J. Feeney, Experimental and computational approaches to estimate solubility and permeability in drug discovery and development settings, Advanced Drug Delivery Reviews 46 (2001) 3–26.